

Pyridine-Pyrazole Based Al(III) ‘Turn on’ Sensor for MCF7 Cancer Cell Imaging And Detection of Picric Acid

Sayan Saha,^{#a} Avik De,^{#a} Arijit Ghosh,^b Avik Ghosh,^c Kaushik Bera,^d Krishna Sundar Das,^a Sohel Akhtar,^a Nakul C. Maiti,^d Abhijit Kumar Das,^c Benu Brata Das,^b and Raju Mondal^{*a}

Table of contents

Fig. S1: Mass spectrum of free ligand.

Fig. S2: Mass spectrum of metal complex.

Fig. S3: Mass spectrum of complex.

Fig. S4: The isotopic distribution of the complex

Fig. S5: Molecular structures of H₂DPC with probability thermal ellipsoids

Fig. S6: Optimized geometry of enol-H₂DPC and keto-H₂DPC

Fig. S7: Images of ligand solution and mixture of different ligand-metal solutions under visible light and UV light (365 nm)

Fig. S8: Plots for determination of binding constant from PL data UV-Vis data

Fig. S9: Step by step addition of EDTA to Zn-H₂DPC complex to eliminate the participation of Zn²⁺ ion in presence of Al³⁺.

Fig. S10: Plot for the determination of limit of detection (LOD)

Table S1: Comparison with few reported chemosensors of Al³⁺

Fig. S11: Jobs plot from UV-Vis data and PL data.

Fig. S12: PL spectra of Al-H₂DPC complex in presence of various counter anion

Fig. S13: PL spectra of Al-H₂DPC complex in presence of inorganic acids

Table S2: Selected bond lengths from theoretical calculations

Fig. S14: Images of ligand-Al³⁺ solution and mixture of ligand-Al³⁺-nitroaromatics solutions under visible light and UV light

Fig. S15: Limit of detection (LOD) for picric acid

Fig. S16: Mass spectrum of metal complex with picric acid

Fig. S17: Cell survival assay with compounds H₂DPC-Al

Scheme S1: Schematic diagram of synthetic procedure

Fig. S18: FT-IR spectrum of free ligand

Fig. S19: NMR spectrum of free ligand

Fig. S20: FT-IR spectrum of ligand-metal complex.

Fig. S21: NMR spectrum of ligand-metal complex.

Table S3: Coordinates of the molecules from theoretical studies

References

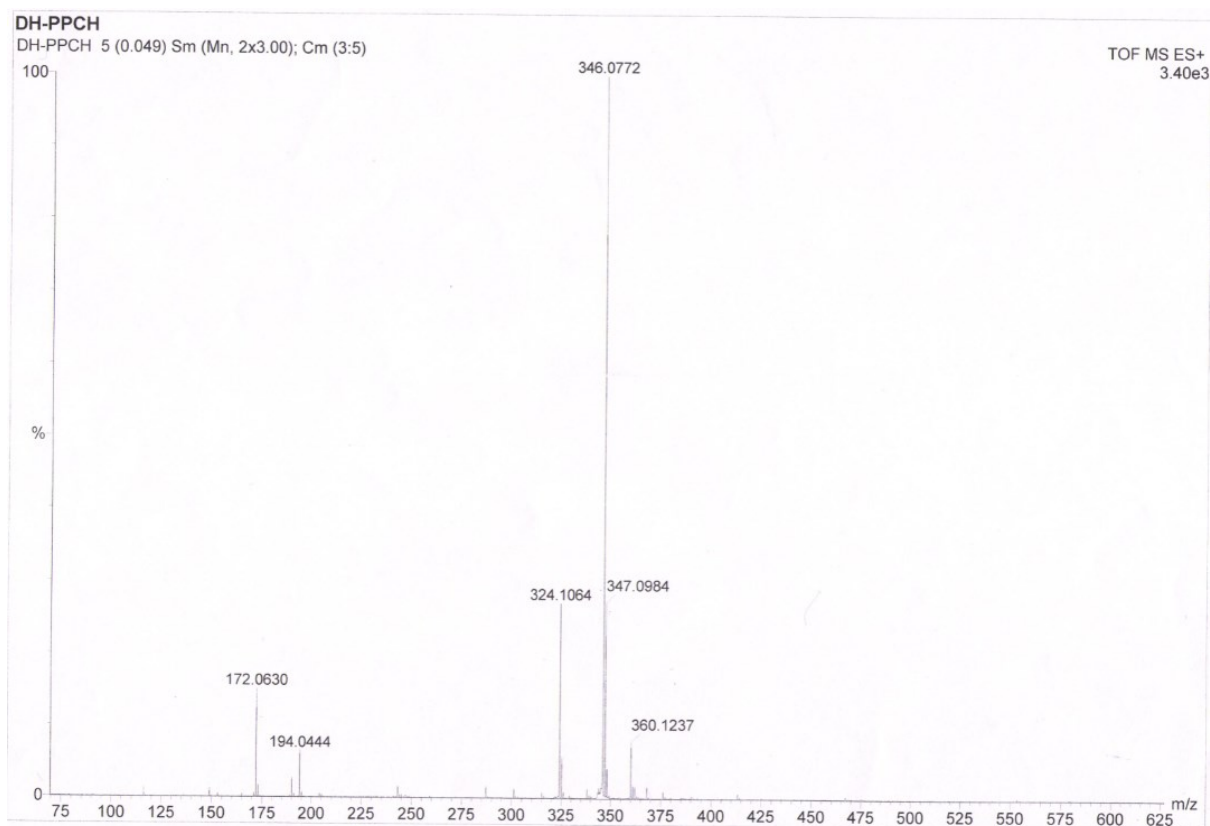


Fig. S1: Mass spectrum of free ligand.

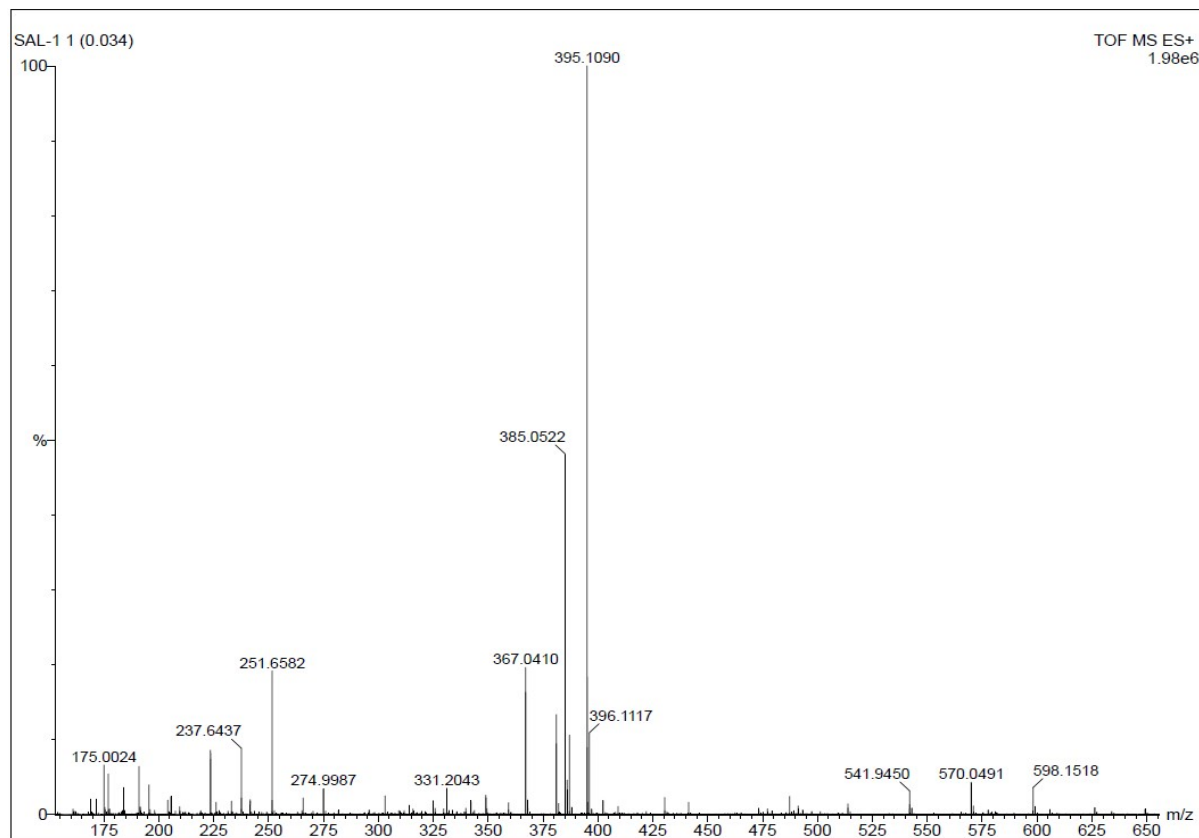


Fig. S2: Mass spectrum of metal complex.

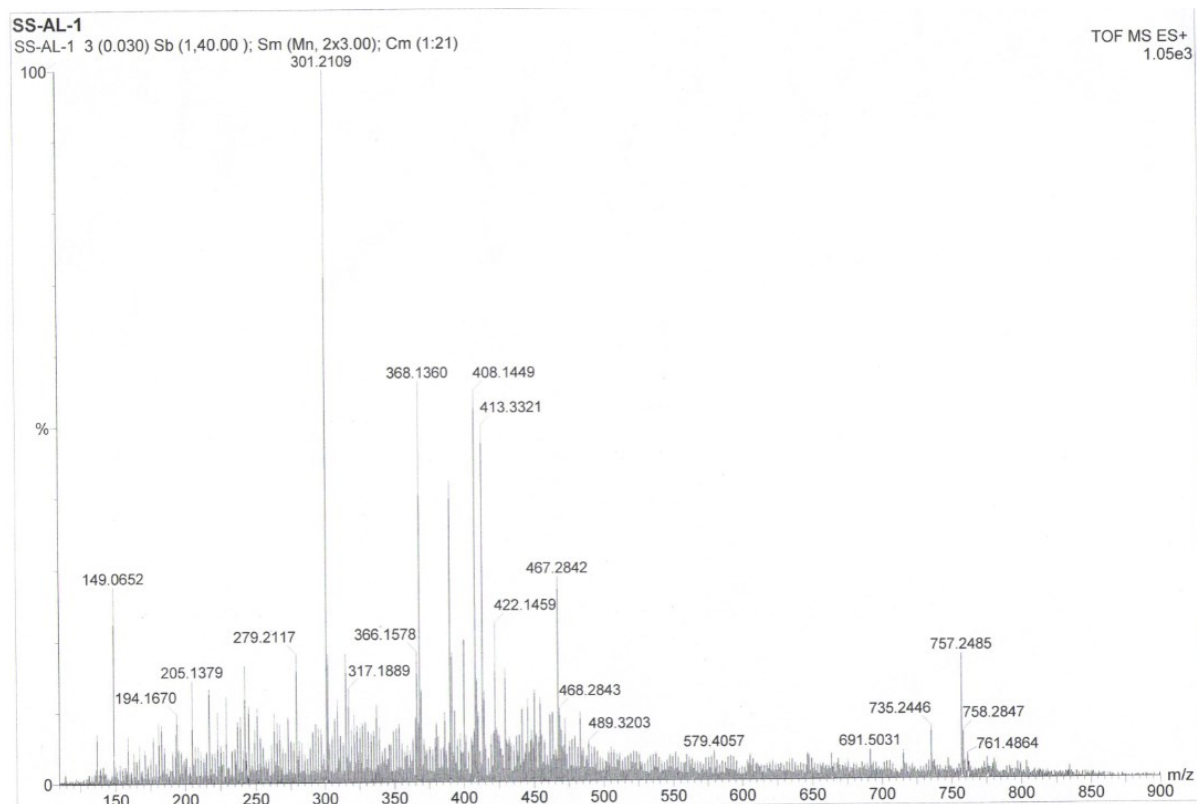


Fig. S3: Mass spectrum of complex.

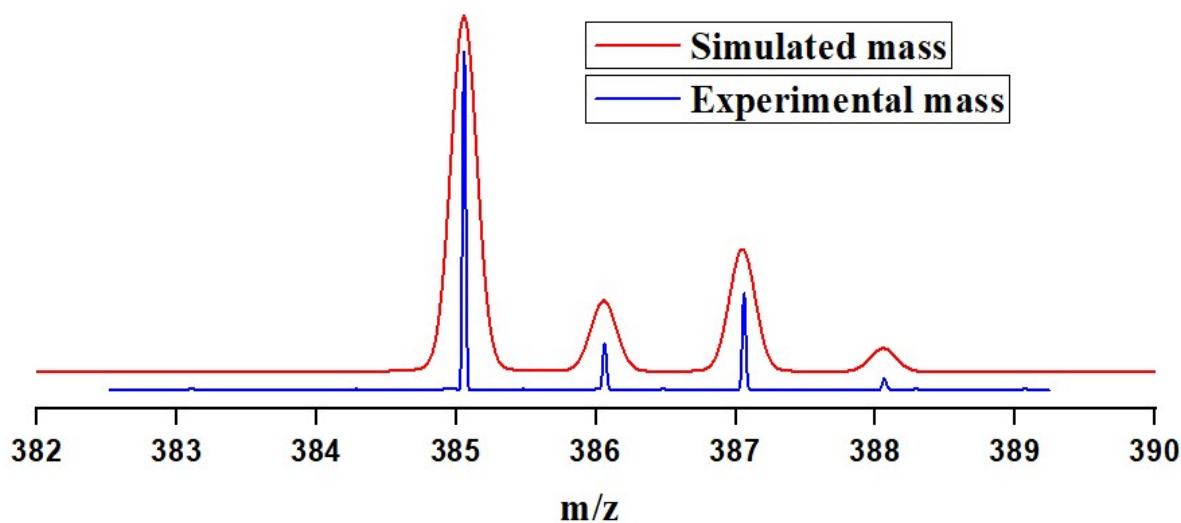


Fig. S4: The isotopic distribution of the complex.

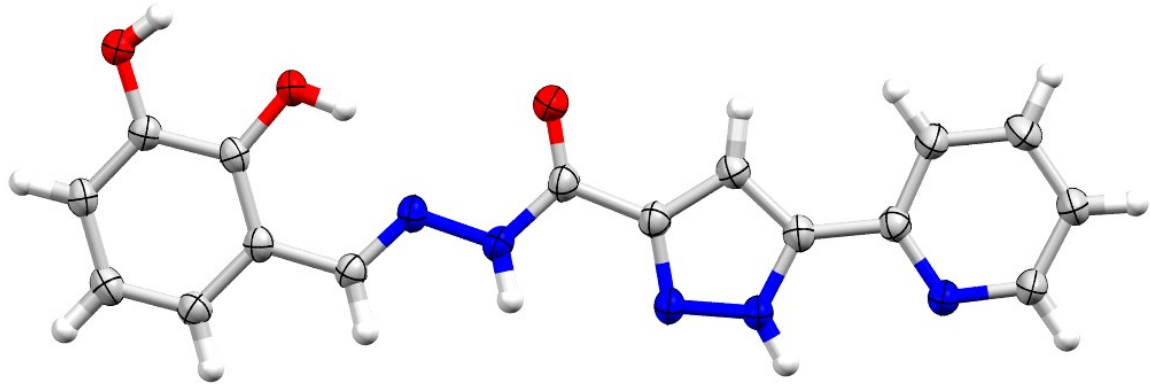


Fig. S5: Molecular structures of H₂DPC with probability thermal ellipsoids.

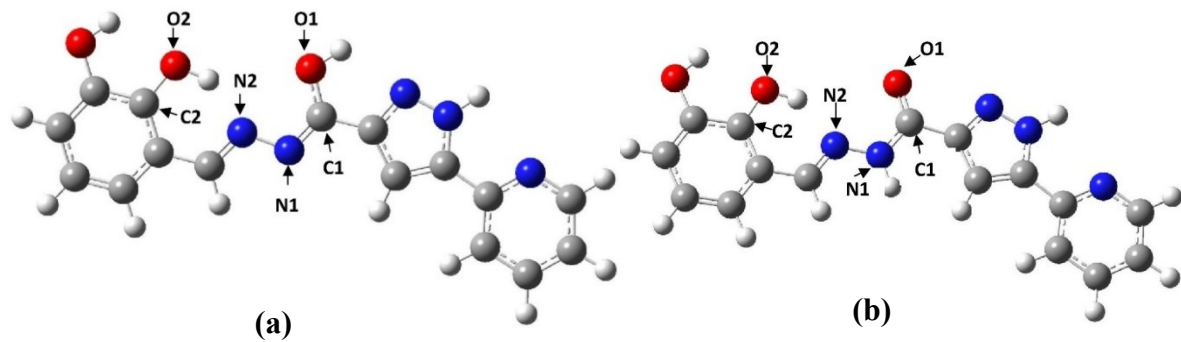
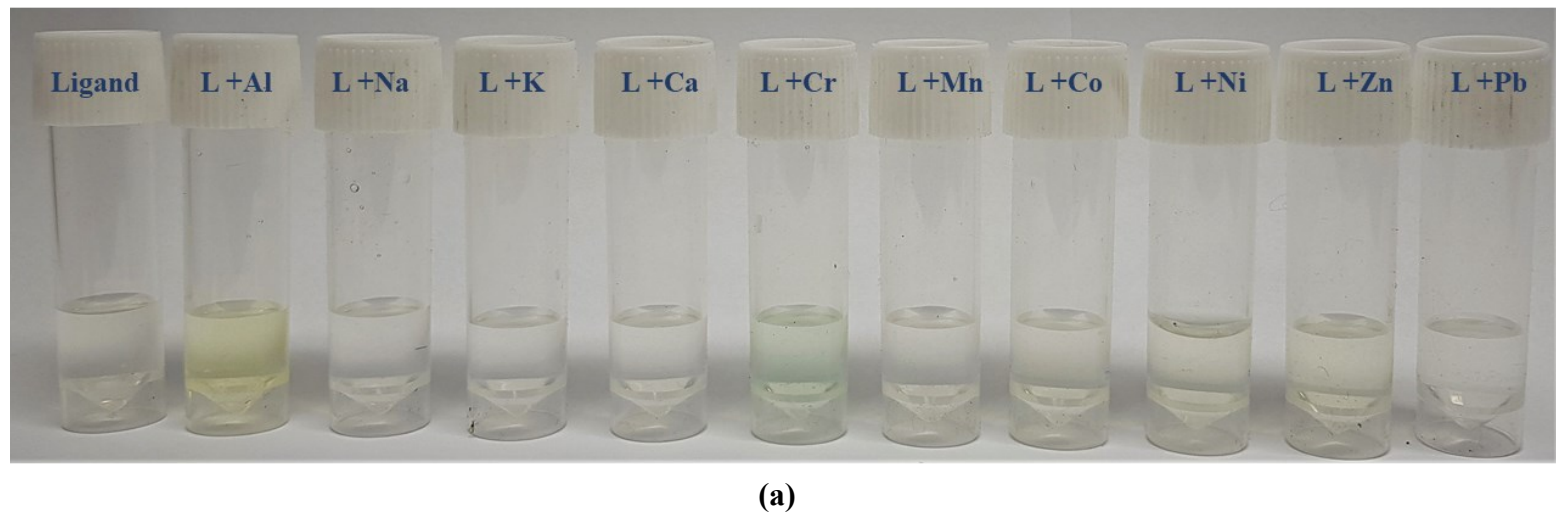
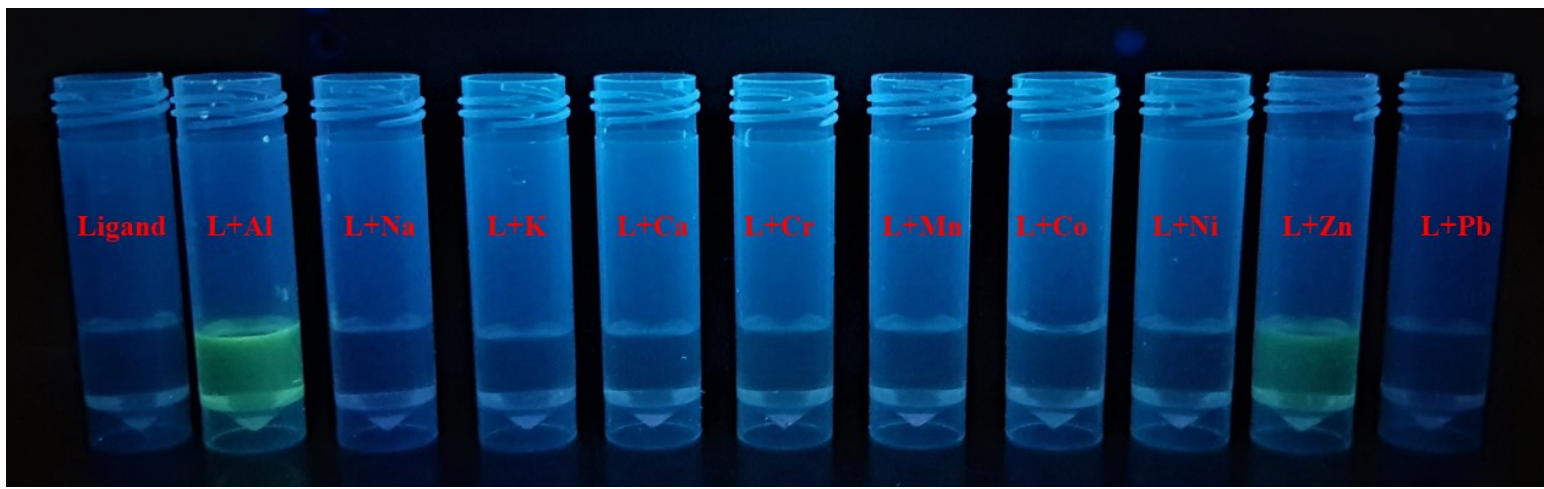


Fig. S6: Optimized geometry of (a) enol-H₂DPC and (b) keto-H₂DPC.





(b)

Fig. S7: Images of ligand solution and mixture of different ligand-metal solutions under (a) visible light and (b) UV light (365 nm).

Binding Constant Evaluation

The binding constant of the ligand metal complex was calculated by using the Benesi-Hildebrand (B-H) plot (equation (1))

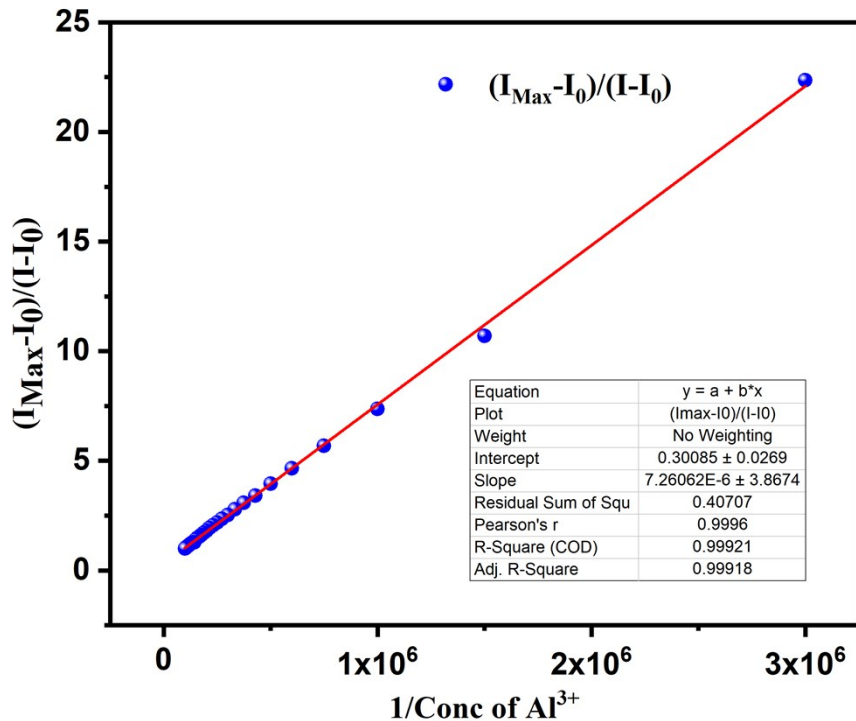
$$1/(I-I_0) = 1/\{K(I_{max}-I_0)[Al^{3+}]\} + 1/(I_{max}-I_0) \quad (1)$$

I_0 is the emission intensity of ligand individually observed at 504 nm, I is the observed emission intensity at 504 nm in the presence of aluminium ions, $[Al^{3+}]$, I_{max} is the maximum value of emission intensity that was obtained at 504 nm during titration with changing Al^{3+} ion concentration, K is the binding constant (M^{-1}) and calculated from the slope of the linear plot. The binding constant was also calculated from the absorption titration experiment using the Benesi-Hildebrand (B-H) plot(equation (2))

$$1/(A-A_0) = 1/\{K_a(A_{max}-A_0)[Al^{3+}]\} + 1/(A_{max}-A_0) \quad (2)$$

where, A_0 and A are the absorbances of L in the absence and presence of Al^{3+} ions respectively and A_{max} is the saturated absorbance of L in the presence of Al^{3+} ions and K_a is the binding

constant and the values come for K_a from PL study is 1.37×10^5 and from the UV study the



value is 3.50×10^5

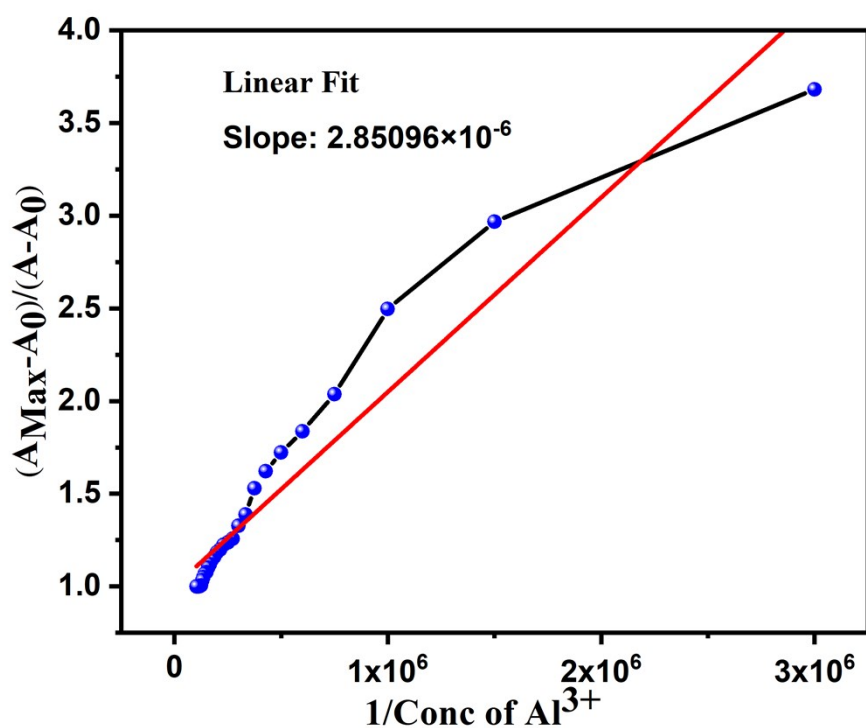


Fig. S8: Plots for determination of binding constant from (a) PL data (b) UV-Vis data.

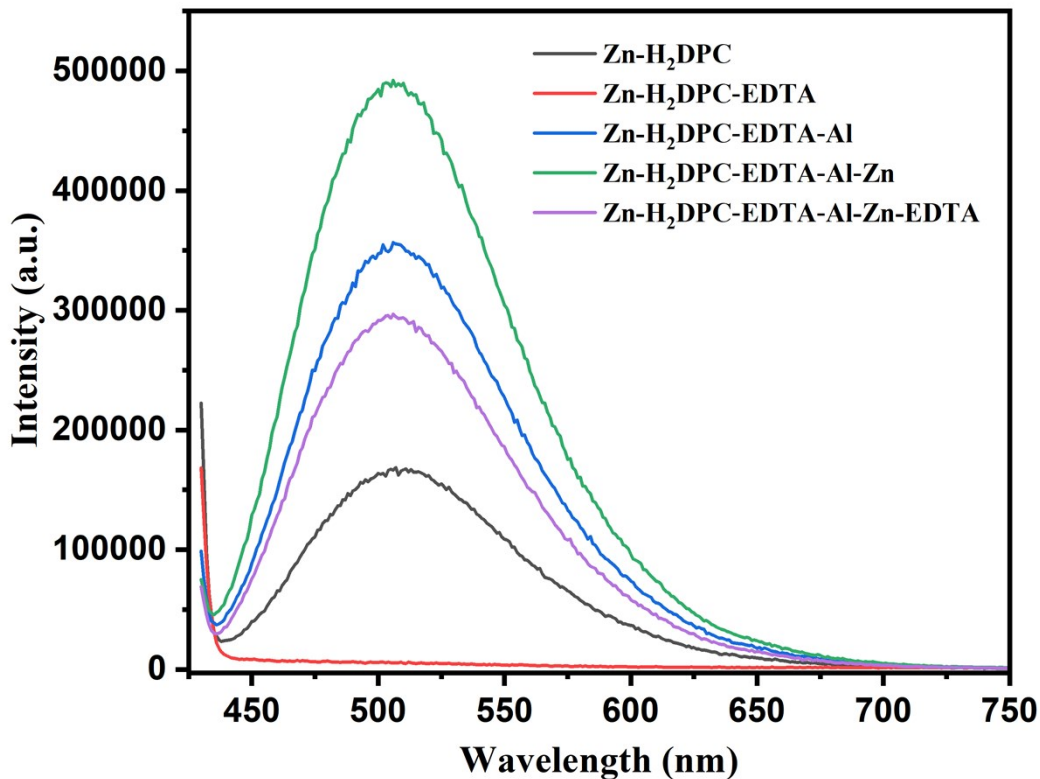


Fig. S9: Step by step addition of EDTA to Zn-H₂DPC complex to eliminate the participation of Zn²⁺ ion in presence of Al³⁺.

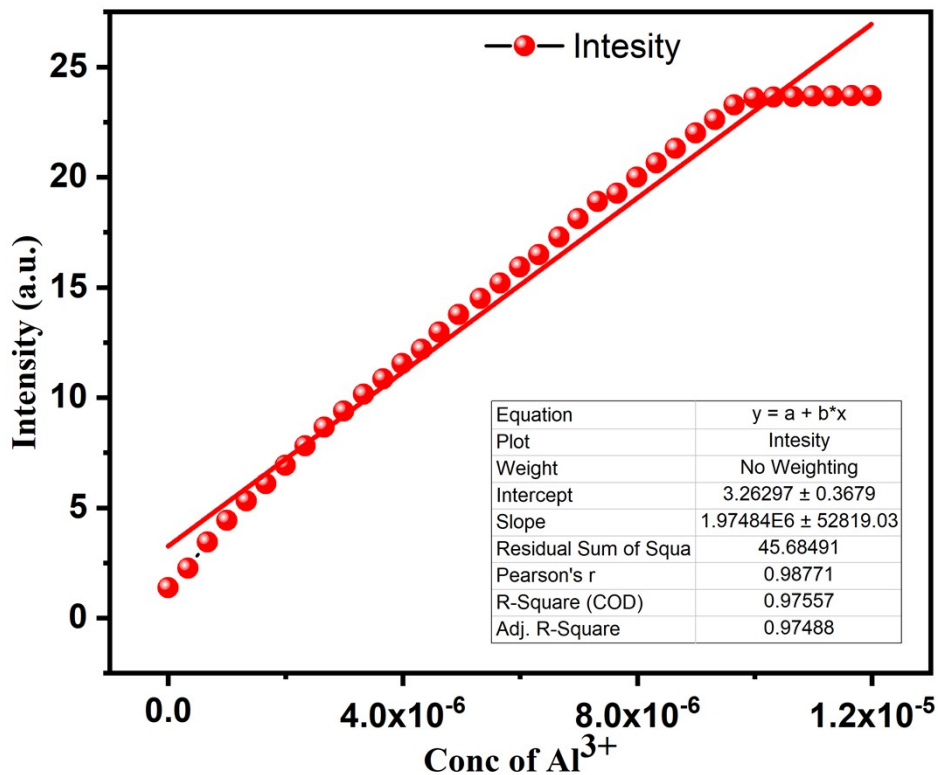
Limit of Detection

On the basis of fluorescence titration experiment the limit of detection was calculated at 503 nm. The fluorescence spectrum of L-Metal complex at the saturation point was measured 8 times to calculate the standard deviation. And to gain the slope the intensity was measured by adding 0.5 μ L of 1.5 molar aqueous aluminium solution into the DMSO solution of ligand repeatedly and plotted the corresponding intensity with respect to the conc. of aluminium salt.

The detection limit was then calculated by making use of the following equation

$$\text{Detection limit} = 3\sigma/k$$

where, σ is the standard deviation of blank measurement, and k is the slope in the plot of



fluorescence emission intensity versus respective analyte concentration for our ligand metal system the standard deviation is 0.141902 and the value of K is 1.97484×10^6 for our system the value of LOD is 2.1565×10^{-7} (M)

Fig. S10: Plot for the determination of limit of detection (LOD).

Table S1: Comparison with few reported chemosensors of Al³⁺

Sample Name.	Excitation(nm)/ Emission(nm)	LOD	Binding Constant (K _a) (M ⁻¹)	Nitro Aromatic Sensing	Cell Imaging	Ref.
N'1,N'3-bis((E)-4-(diethylamino)-2-hydroxybenzylidene)-isophthalohydrazide (NDHIPH)	(λ _{ex} 383 nm)/(λ _{em} 485 nm)	2.53 nM	4.25×10 ¹² M ⁻¹	YES	NO	1
2-Quinolinecarboxylic acid, 2-[4-(diethylamino)-2-hydroxyphenyl]methylene]hydrazide	(λ _{ex} 390 nm)/(λ _{em} 480 nm), (λ _{ex} 440 nm)/(λ _{em} 590 nm)	0.104μM at 480nm, 4.17μM at 590 nm	1.67 × 10 ⁵ M ⁻¹ for the 590 nm emission	NO	YES	2
5-(diethylamino)-2-(1 <i>H</i> -phenanthro[9,10- <i>d</i>]imidazol-2-yl)-Phenol	(λ _{ex} 375 nm)/(λ _{em} 412nm)	0.5 nM	3.36 × 10 ⁵ M ⁻¹	NO	NO	3
(E)-4-(((2-hydroxynaphthalen-1-yl)methylene)amino)-N-(5-methylisoxazol-3-yl)benzenesulfonamide	(λ _{ex} 360 nm)/(λ _{em} 450 nm)	33.2 nM	1.04 + 0.01) ×10 ⁴ M ⁻¹	NO	YES	4
1-[(8-quinolinylimino)methyl]-2-Naphthalenol,	(λ _{ex} 320 nm.)/(λ _{em} 520 nm)	1.0 μM	5.01 × 10 ⁸ M ⁻¹	NO	NO	5

4-(8'-hydroxyquino-lin-5'-yl)methyleneimino-1-phenyl-2,3-dimethyl-5-pyzole	(λ_{ex} 378nm.)/(λ_{em} 470 nm)	0.1 μM	$\log \beta = 6.8$	NO	NO	6
2-[1-(2-pyrazinyl) ethylidene] hydrazide Benzoic acid,	(λ_{ex} 390nm.)/(λ_{em} 506 nm)	0.1 μM	$1.24 \times 10^7 \text{ M}^{-1}$	NO	NO	7
1-[(2-pyridinylmethyl) imino]methyl]- 2-Naphthalenol,	(λ_{ex} 355nm.)/(λ_{em} 432 nm,370 nm)	0.648 mM	$1 \times 10^5 \text{ M}^{-1}$	NO	NO	8
[4-amino-3-[(2-hydroxyphenyl) methylene]amino] phenyl]phenyl-Methanone	(λ_{ex} 334nm.)/(λ_{em} 502 nm)	8.12 μM	$1 \times 10^4 \text{ M}^{-1}$	NO	NO	9
NPRB.	(λ_{ex} 490nm.)/(λ_{em} 578 nm)	0.3 μM		NO	YES	10
(E)-N'-(2,3-dihydroxybenzylidene)-3-(pyridin-2-yl)-1H-pyrazole-5-carbohydrazide (H₂DPC)	(λ_{ex} 417 nm)/(λ_{em} 504 nm)	0.215 μM	$1.37 \times 10^5 \text{ M}^{-1}$	YES	YES	Our result

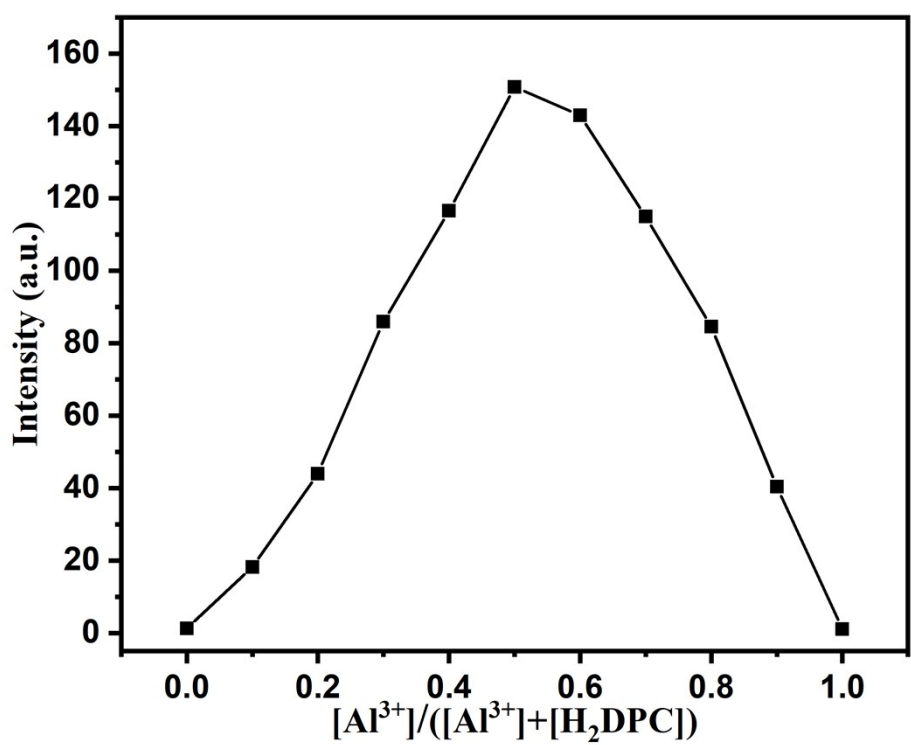
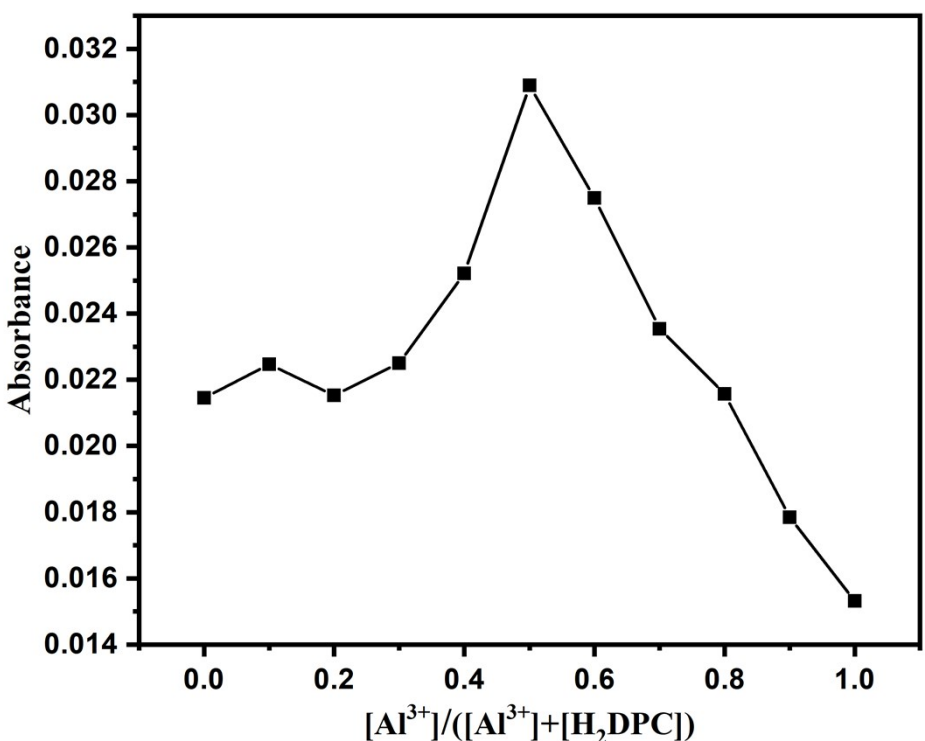


Fig. S11: Jobs plot from (a) UV-Vis data and (b) PL data.

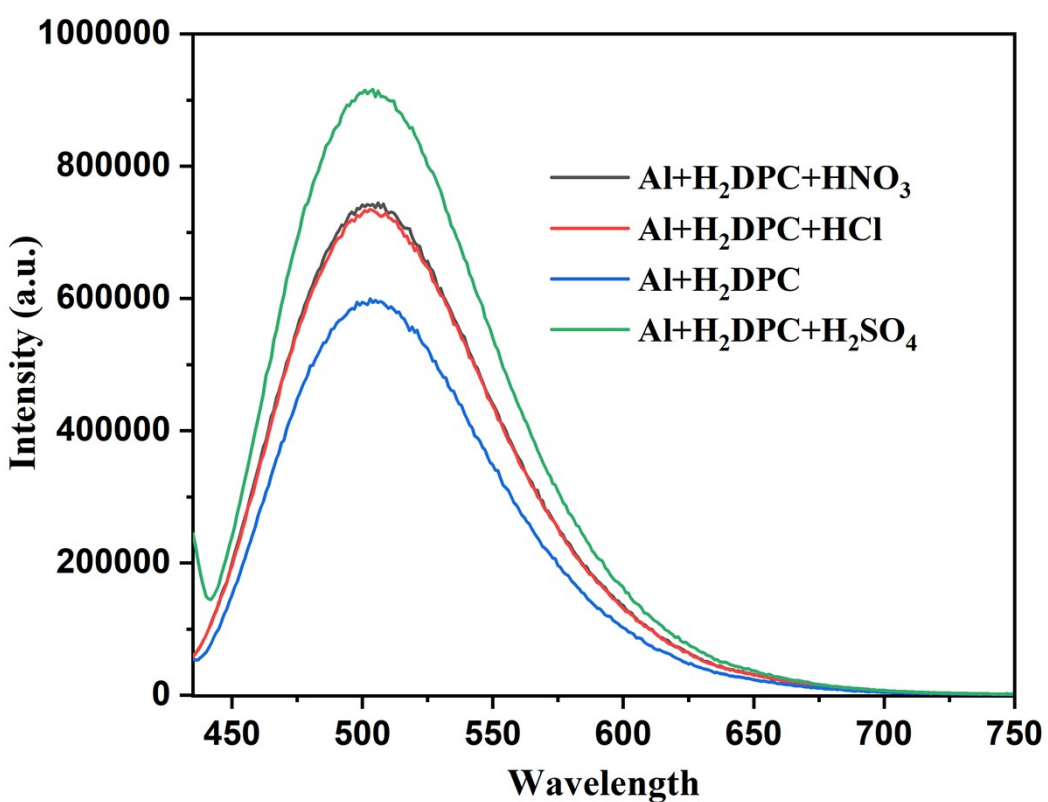
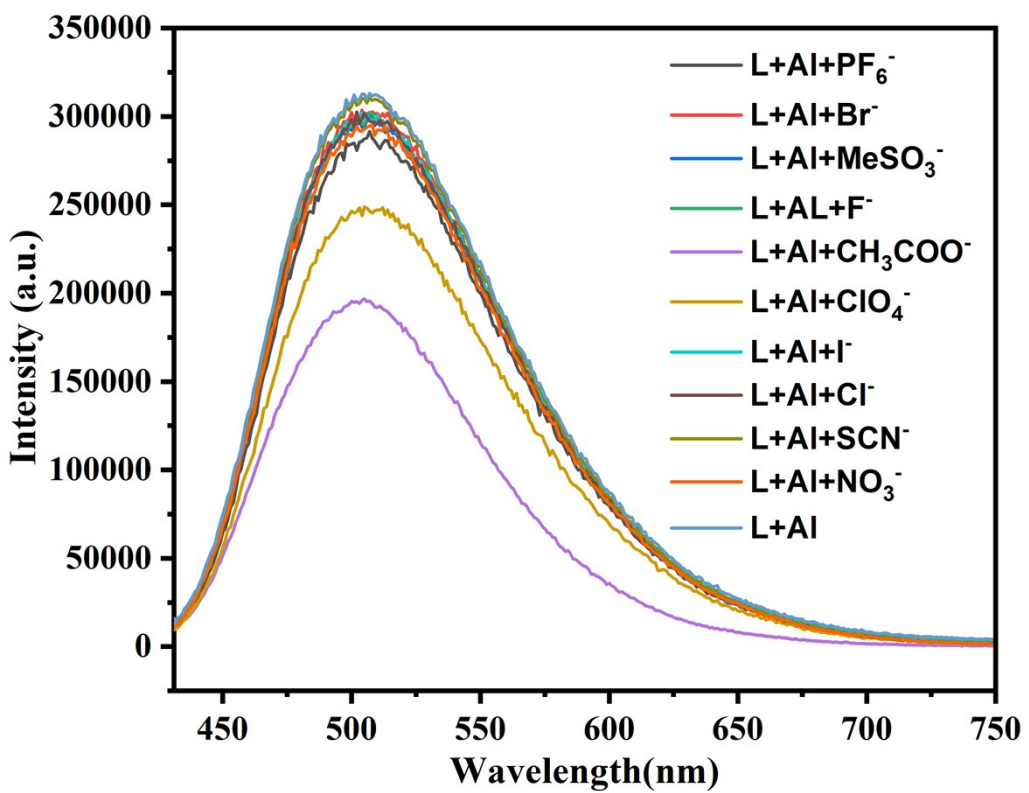
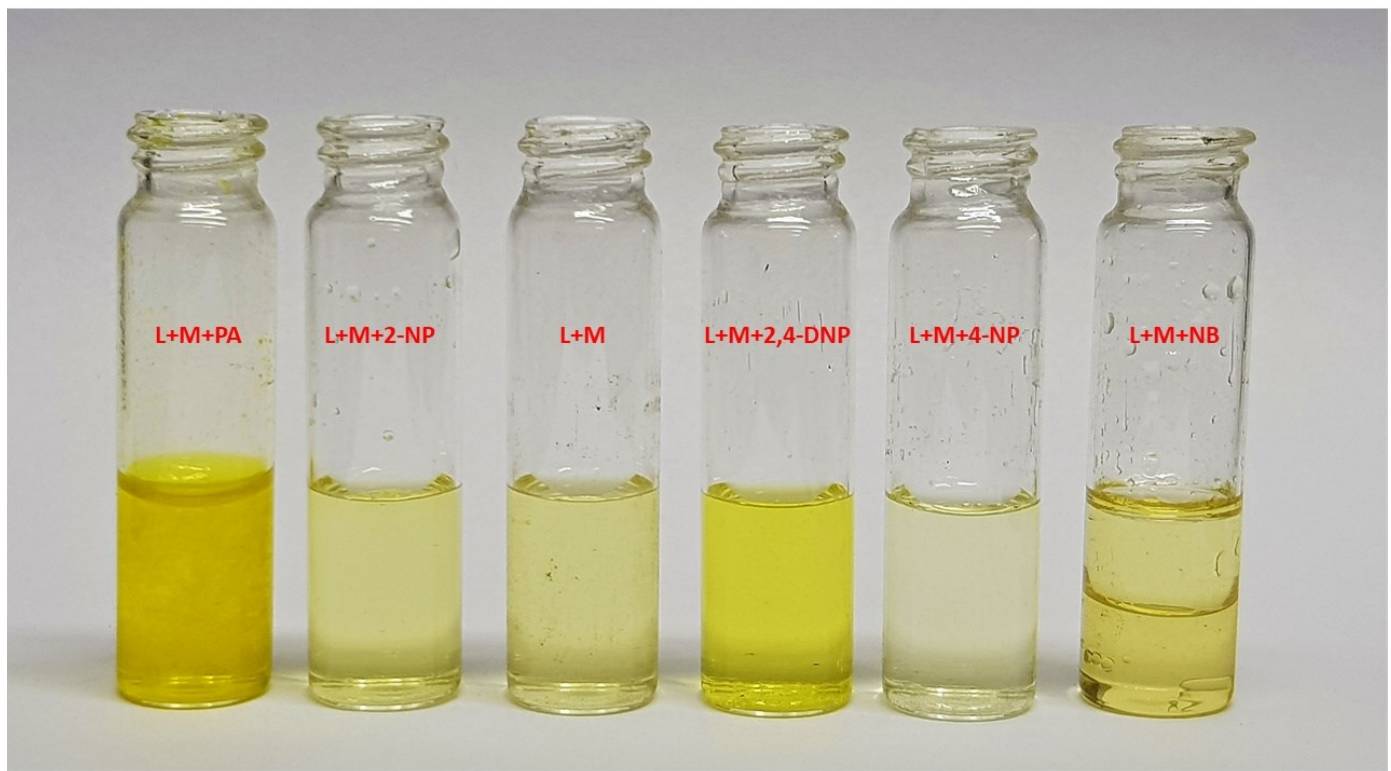


Fig. S12: PL spectra of Al-H₂DPC complex in presence of various counter anion.

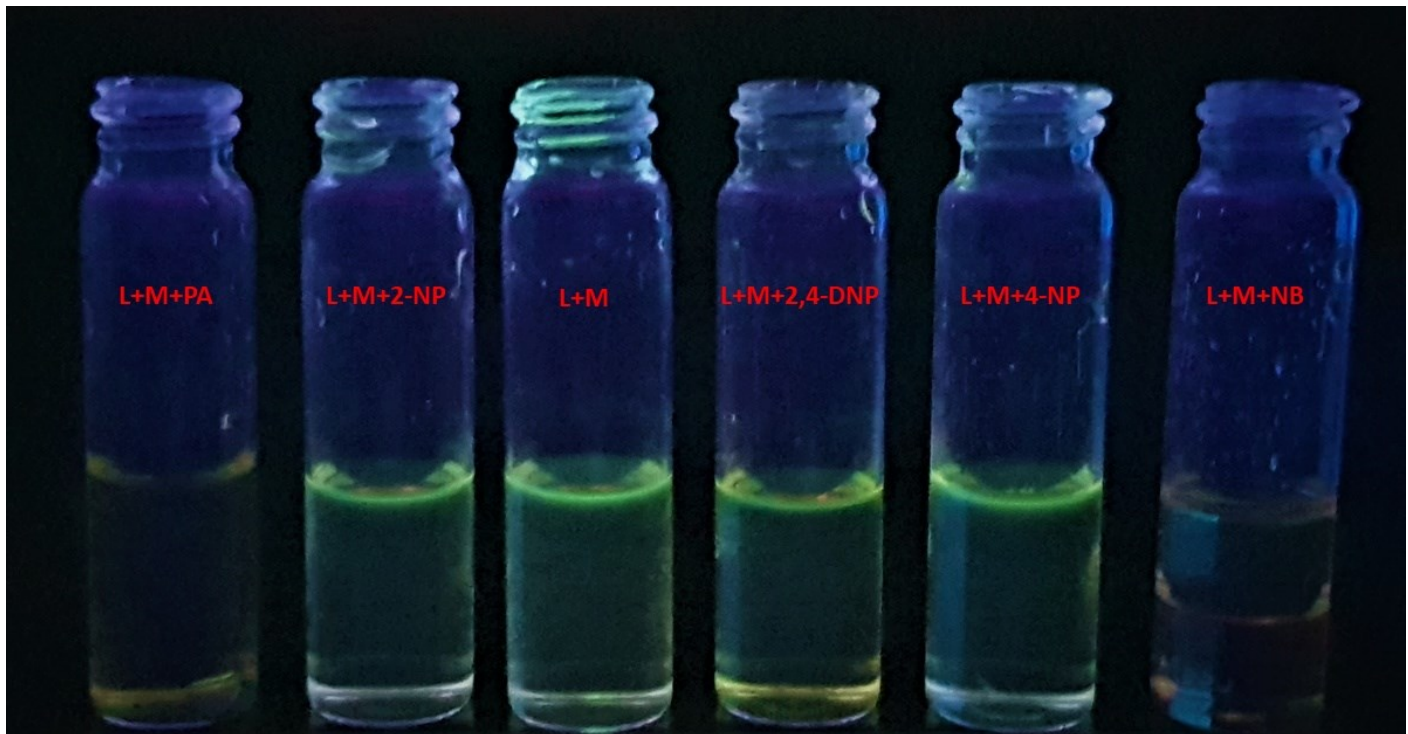
Fig. S13: PL spectra of Al-H₂DPC complex in presence of inorganic acids.

Table S2: Selected bond lengths from theoretical calculations

Molecule	O1-C1	C1-N1	N1-N2	O2-C2	Al-O2	Al-O1	Al-Cl
keto-DHPCH	1.23	1.37	1.36	1.35	-	-	-
enol-DHPCH	1.34	1.28	1.38	1.35	-	-	-
Al-DHPCH	1.31	1.31	1.39	1.34	1.80	1.85	2.22



(a)



(b)

Fig. S14: Images of ligand- Al^{3+} solution and mixture of ligand- Al^{3+} -nitroaromatics solutions under (a) visible light and (b) UV light.

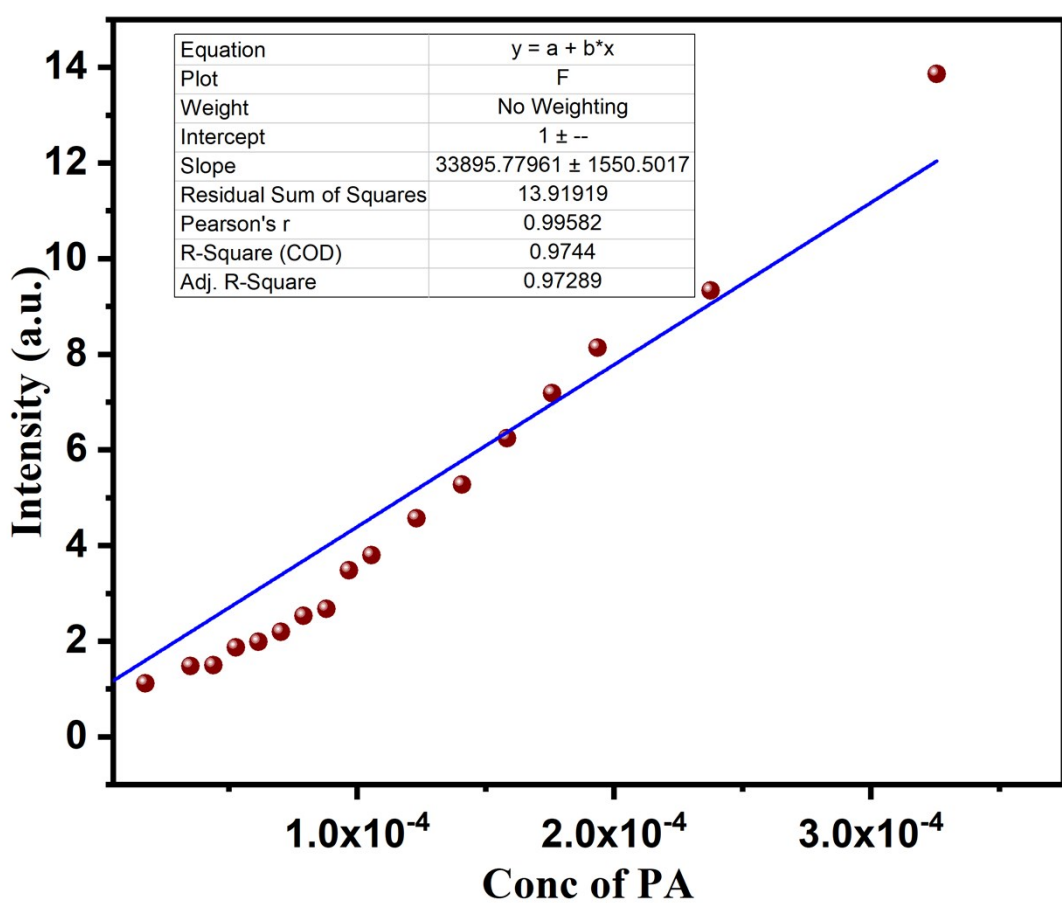


Fig. S15: Limit of detection (LOD) for picric acid.

Detection limit = $3\sigma/k$ Standard deviation=1.384999, Slope =33895.77

$$\text{LOD} = 1.2257 \times 10^{-4} (\text{M})$$

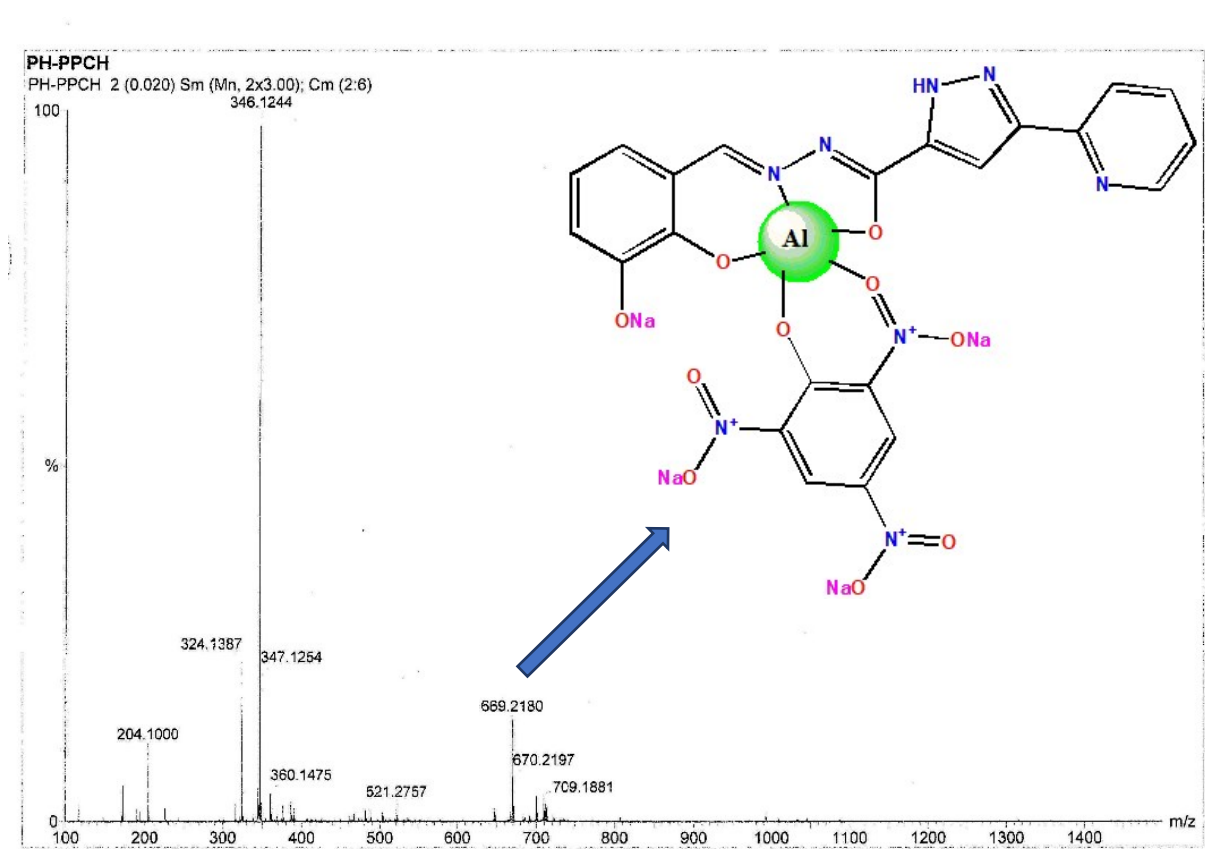


Fig. S16: Mass spectrum of metal complex with picric acid.

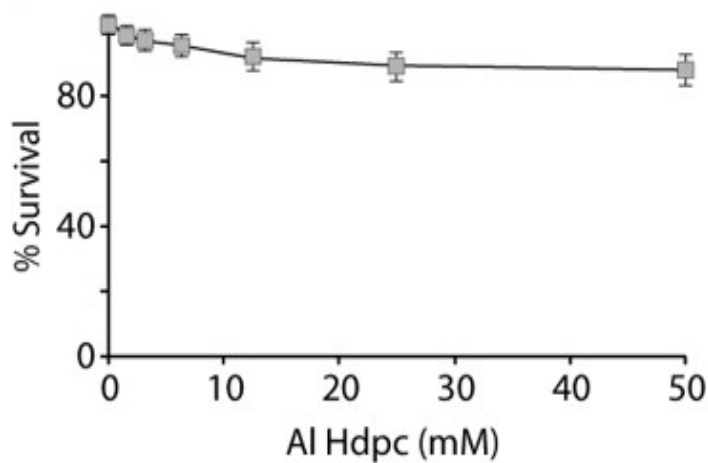
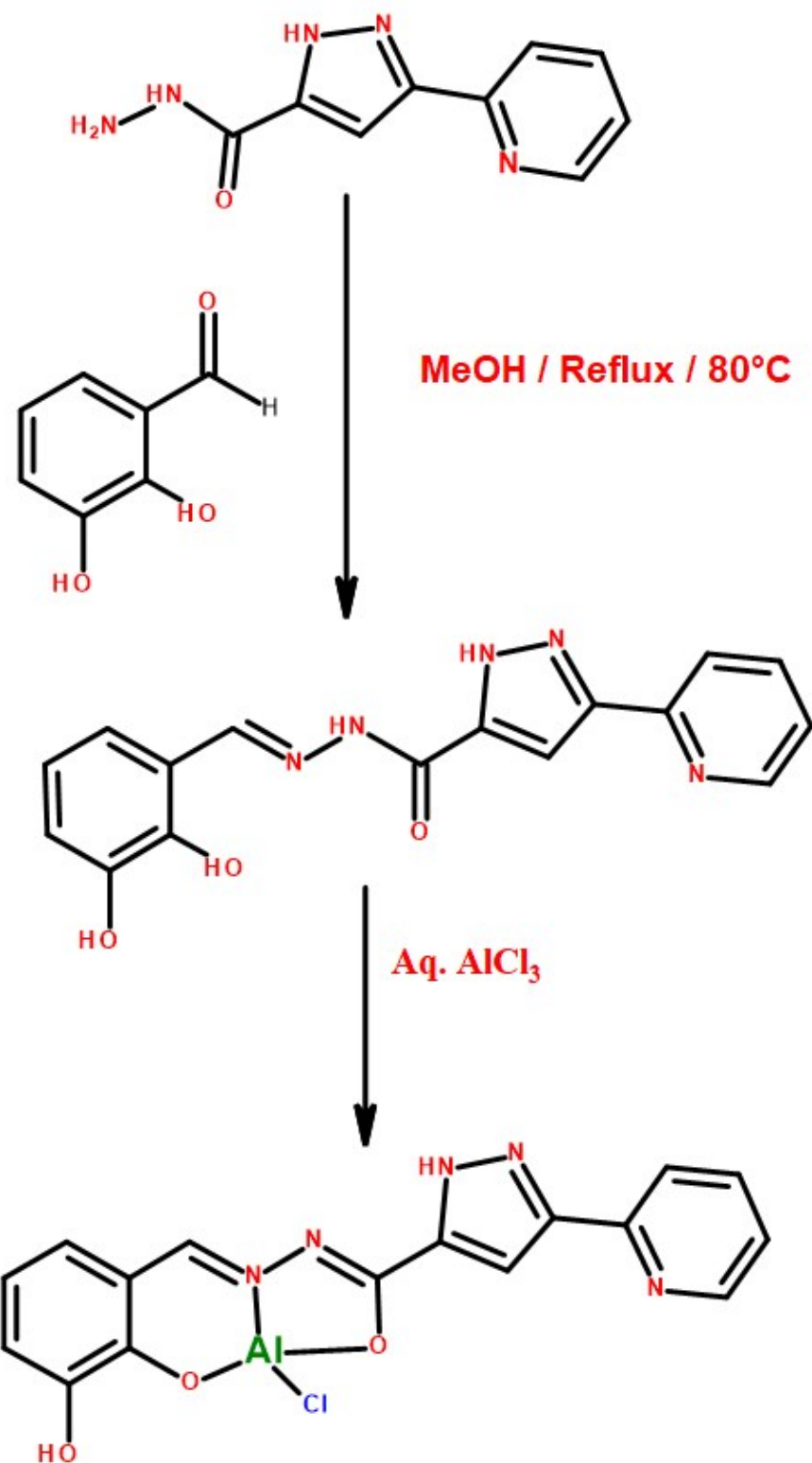


Fig. S17: Cell survival assay with compounds H₂DPC-Al reveals no apparent cytotoxicity. Survival curves of MCF7 cells treated with H₂DPC-Al for 72 hrs. Cell viability was determined by MTT assays. Errors bars represent standard deviation (n≥3).



Scheme S1: Schematic diagram of synthetic procedure.

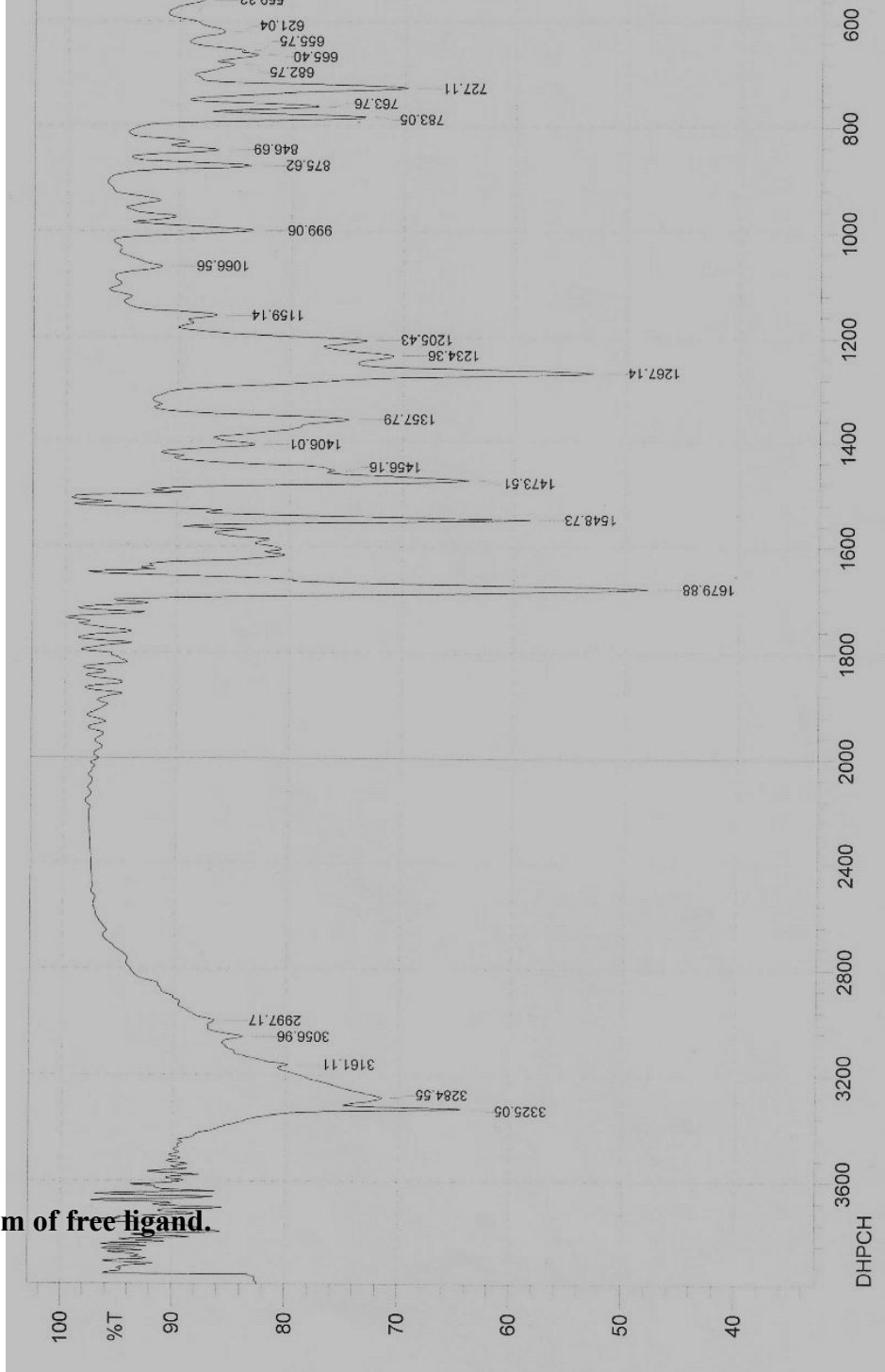


Fig. S18: FT-IR spectrum of free ligand.

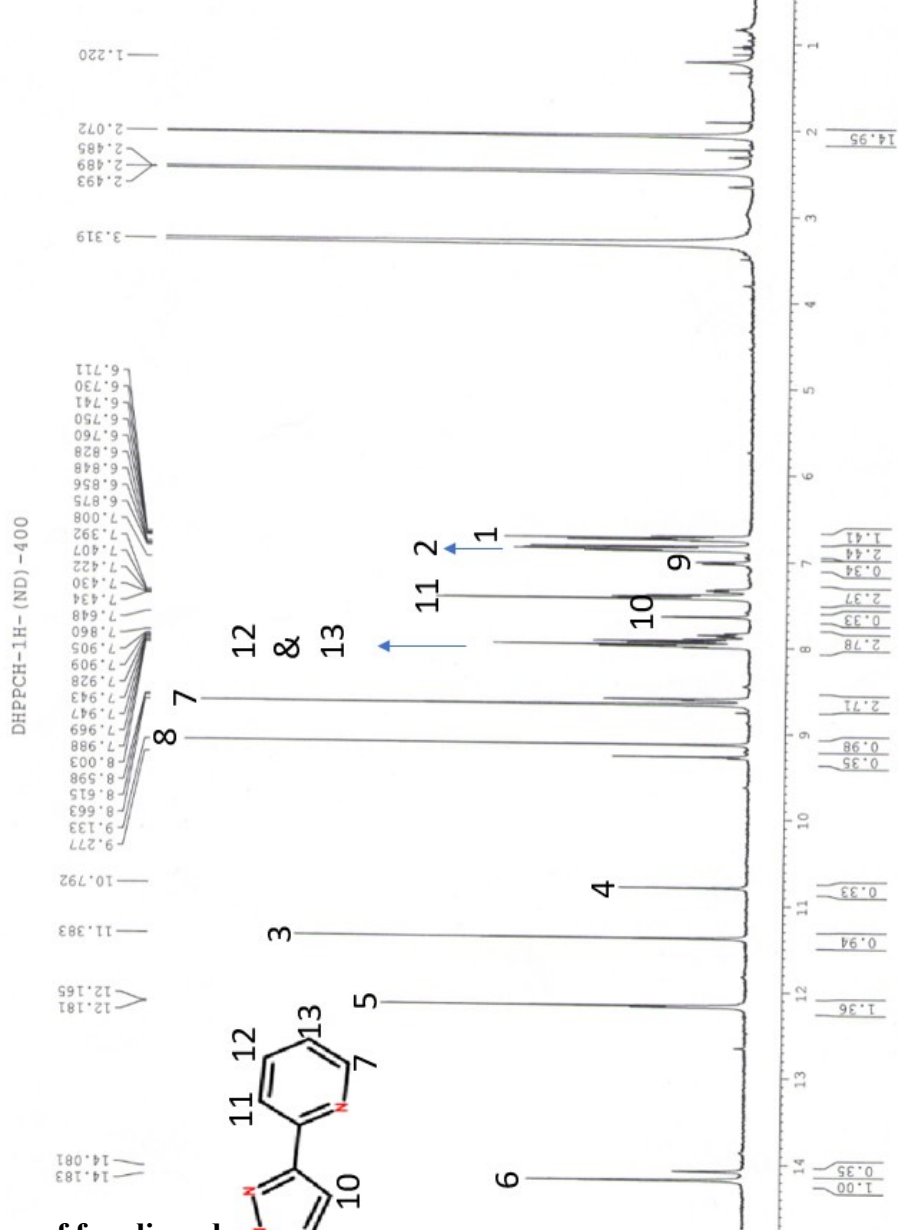
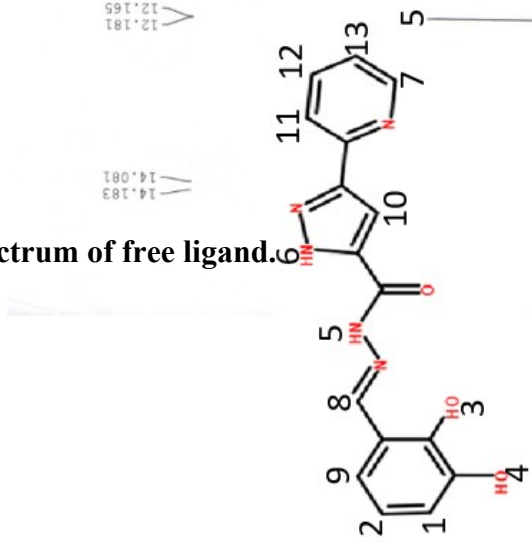
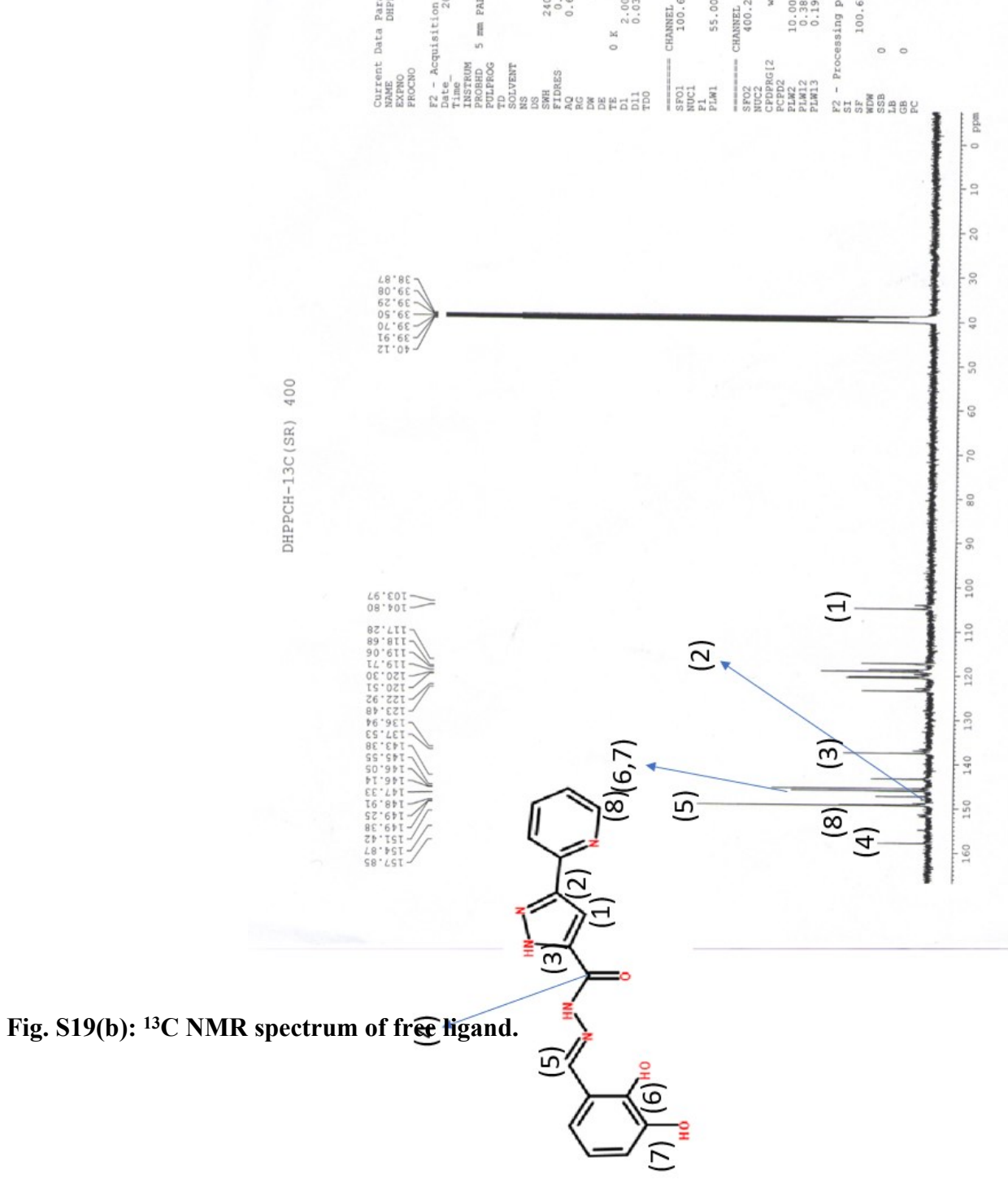


Fig. S19(a): ^1H NMR spectrum of free





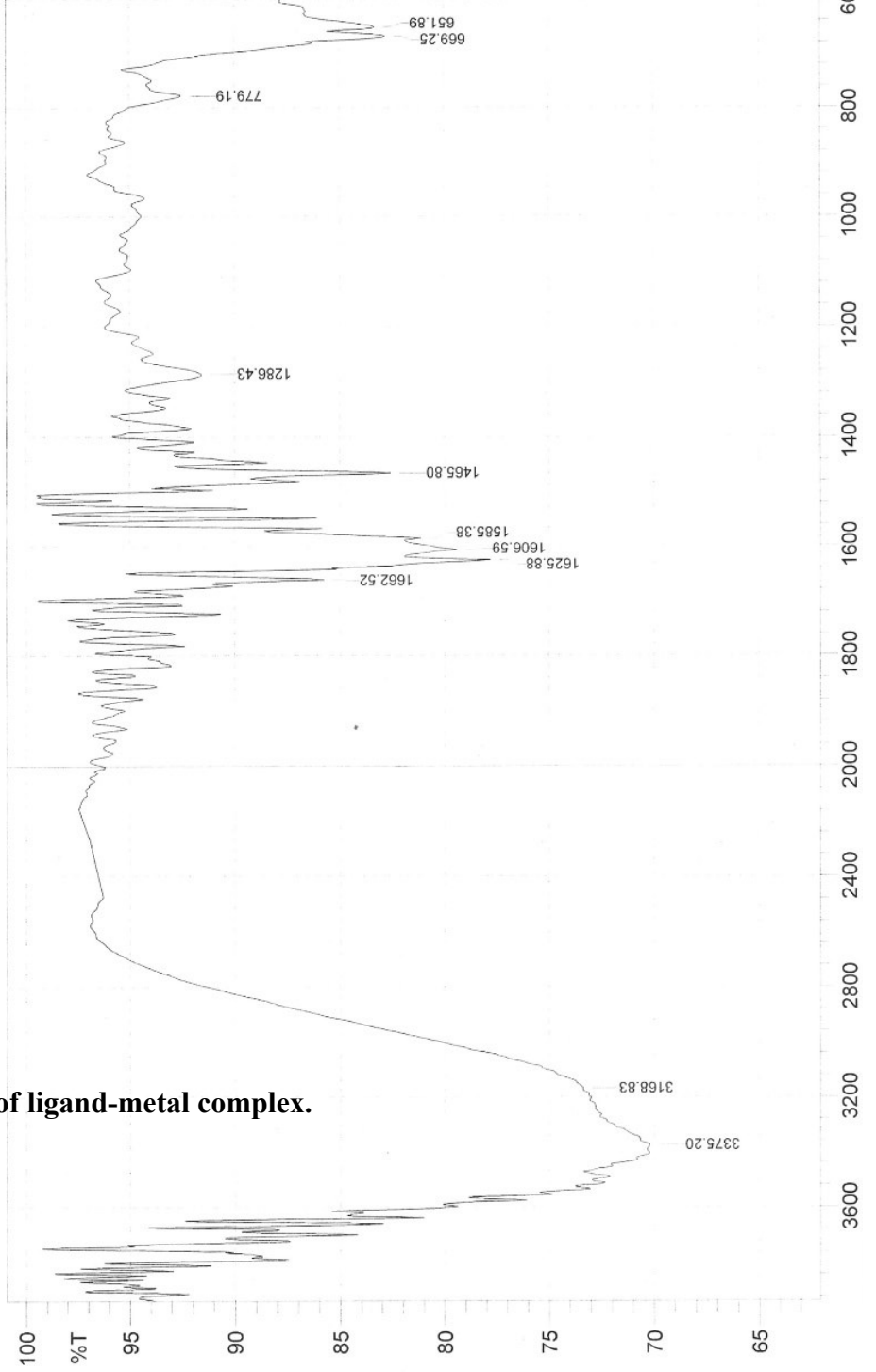


Fig. S20: FT-IR spectrum of ligand-metal complex.

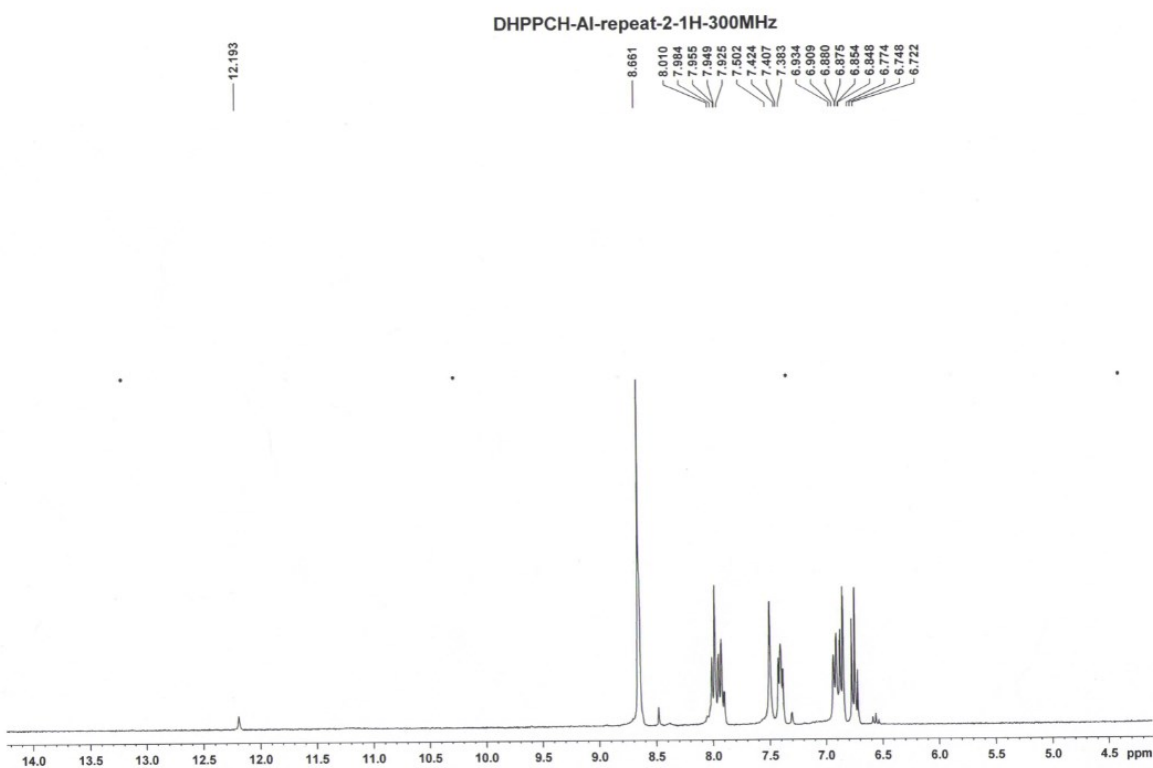


Fig. S21: ¹H NMR spectrum of ligand-metal complex.

Table S3: Coordinates of the molecules from theoretical studies**keto-DHPCH**

C	-6.81719700	1.12258900	-0.00027600
C	-6.18043300	-0.10766700	-0.00004700
C	-4.78205000	-0.17984500	0.00015700
C	-4.02045700	0.99918900	0.00011700
C	-4.68018200	2.23927700	-0.00014900
C	-6.06389900	2.29983400	-0.00032600
H	-7.90205300	1.15154500	-0.00043200
H	-4.08762500	3.14896200	-0.00021100
H	-6.56851300	3.25981500	-0.00049700
O	-6.91874700	-1.25478900	-0.00006800
H	-6.32143100	-2.01945300	0.00036800
O	-4.24261000	-1.42328000	0.00043300
C	-2.56510000	0.96014700	0.00022800
N	-1.94101200	-0.16096000	-0.00000100
H	-2.02940400	1.91328900	0.00040900
N	-0.58029500	-0.13439300	-0.00009000
C	0.12309800	-1.30018200	0.00000900
O	-0.41826200	-2.40381100	0.00009000
H	-0.10622100	0.76377000	0.00002100
C	3.68776600	-0.40939300	-0.00000700
C	2.38193000	0.04273200	0.00006500
C	1.59812000	-1.13084500	-0.00001200
H	2.05581200	1.07195700	0.00009800
N	2.36605900	-2.22277000	-0.00009700
N	3.61180000	-1.76235300	-0.00003900
C	7.26886100	0.07333900	-0.00036700
C	7.45024700	1.45257300	-0.00003800
C	6.32206700	2.26571100	0.00033500
C	5.06513400	1.67536900	0.00036000
C	4.98364400	0.28263300	-0.00001200
N	6.06716300	-0.50706600	-0.00036400
H	6.41797200	3.34659400	0.00061000
H	8.12527900	-0.59549100	-0.00065800
H	8.45019500	1.87148000	-0.00007000
H	4.16642300	2.28164500	0.00067000
H	4.39777500	-2.40084100	-0.00013500
H	-3.25655200	-1.33822100	0.00010200

enol-DHPCH

C	-6.90517600	0.93546900	0.00066000
C	-6.18079100	-0.24472000	0.00048600
C	-4.78048800	-0.21327100	0.00012700
C	-4.10757000	1.01986000	0.00000100
C	-4.85678000	2.20891000	0.00018300
C	-6.24069700	2.16644800	0.00050100
H	-7.98933300	0.88519000	0.00093000
H	-4.33222600	3.15933700	0.00009100
H	-6.81600400	3.08585200	0.00064000
O	-6.83028700	-1.44489100	0.00063900
H	-6.17470600	-2.16042500	0.00063300

O	-4.14314200	-1.40625600	-0.00004200
C	-2.65465200	1.07270300	-0.00025300
N	-1.95922000	-0.00921700	-0.00040200
H	-2.16507300	2.04929400	-0.00027800
N	-0.58910500	0.18513800	-0.00059700
C	0.09228300	-0.90402600	-0.00058300
O	-0.46542000	-2.12147000	-0.00047300
C	3.69617300	-0.32689400	-0.00040200
C	2.43621400	0.24370400	-0.00043700
C	1.55748300	-0.85509100	-0.00069800
H	2.18324100	1.29232100	-0.00015000
N	2.22135400	-2.01209100	-0.00092200
N	3.50597800	-1.66939600	-0.00075300
C	7.30622900	-0.16076100	0.00234500
C	7.60713300	1.19757200	0.00103200
C	6.55440900	2.10620800	-0.00091100
C	5.25070900	1.62770500	-0.00145300
C	5.04844100	0.24759600	0.00004400
N	6.05854500	-0.63403700	0.00189100
H	6.74430700	3.17459100	-0.00203400
H	8.10108100	-0.90162700	0.00385000
H	8.63984100	1.52766400	0.00150700
H	4.40740500	2.30881000	-0.00307300
H	4.23211600	-2.37493500	-0.00084500
H	-3.15976500	-1.22182200	-0.00020400
H	0.23952800	-2.79455100	-0.00043000

Al-DHPCH

C	6.52193000	1.45060200	-0.19574300
C	5.80737300	0.28075500	-0.36427000
C	4.40442400	0.25625600	-0.22564400
C	3.73534100	1.45925800	0.08347200
C	4.47957800	2.64759700	0.24554900
C	5.85319500	2.64345500	0.11229000
H	7.60132500	1.42881000	-0.30797700
H	3.94909800	3.56708100	0.47270600
H	6.41939400	3.55957900	0.23916700
O	6.44807400	-0.88223600	-0.66997900
H	5.77129600	-1.57804100	-0.73808700
O	3.82236800	-0.93129300	-0.40820300
C	2.29714400	1.53779900	0.16960300

N	1.53656300	0.50125200	0.07059000
H	1.83111500	2.51596700	0.28669400
N	0.16023700	0.67682600	0.04442700
C	-0.39178200	-0.44337000	-0.34380900
O	0.29426000	-1.51491000	-0.65011600
C	-4.02313800	-0.10960900	-0.26123700
C	-2.79205300	0.46935900	-0.02080000
C	-1.85686300	-0.50858600	-0.41686600
H	-2.58881900	1.44580200	0.39008200
N	-2.46475900	-1.60714400	-0.87132400
N	-3.76496800	-1.34049300	-0.76855900
C	-7.63715800	-0.13884400	-0.19287500
C	-8.00085000	1.10527600	0.31182800
C	-6.99117100	2.00335500	0.64151100
C	-5.66745800	1.62700800	0.45744100
C	-5.40035400	0.35583700	-0.05253100
N	-6.36903100	-0.51372600	-0.37426600
H	-7.22994900	2.98503500	1.03754300
H	-8.39656000	-0.86782800	-0.46249000
H	-9.04738100	1.35745400	0.44077300
H	-4.85670400	2.30297100	0.70442000
H	-4.45629900	-2.02375800	-1.05043100
Al	2.08273500	-1.34840700	-0.19300100
Cl	1.98206300	-2.49236300	1.70173000

References

1. S. Sharma, G. Dubey, B. S. Sran, P. V. Bharatam, and G. Hundal, Fabrication of a Hydrazone-Based Al(III)-Selective “Turn-On” Fluorescent Chemosensor and Ensuing Potential Recognition of Picric Acid, *ACS Omega*, 2019, **4**, 18520–18529.
2. R. Singh, S. Samanta, P. Mullick, A. Ramesh, G. Das, Al³⁺ sensing through different turn-on emission signals vis-à-vis two different excitations: Applications in biological and environmental realms, *Anal. Chim. Acta*, 2018, **1025**, 172-180.
3. S. Sinha, B. Chowdhury, and P. Ghosh, A Highly Sensitive ESIPT-Based Ratiometric Fluorescence Sensor for Selective Detection of Al³⁺, *Inorg. Chem.* 2016, **55**, 9212–9220.
4. S. Mondal, A. K. Bhanja, D. Ojha, T. K. Mondal, D. Chattopadhyay and C. Sinha, Fluorescence sensing and intracellular imaging of Al³⁺ ions by using naphthalene based sulphonamide chemosensor: structure, computation and biological studies, *RSC Adv.*, 2015, **5**, 73626-73638.
5. H. M. Park, B. N. Oh, J. H. Kim, W. Qiong, I. H. Hwang, K. -D Jung, C. Kim, J. Kim, Fluorescent chemosensor based-on naphthol-quinoline for selective detection of aluminum ions, *Tet. Lett.*, 2011, **52**, 5581-5584.

- 6.** X. -H. Jiang, B.-D. Wang, Z. -Y. Yang, Y. -C. Liu, T. -R. Li, Z.-C. Liu, 8-Hydroxyquinoline-5-carbaldehyde Schiff-base as a highly selective and sensitive Al^{3+} sensor in weak acid aqueous medium, *Inorg. Chem Comm.*, 2011, **14**, 1224-1227.
- 7.** Z. -C. Liao, Z. -Y. Yang, Y. Li, B. -D. Wang, Q. -X. Zhou, A simple structure fluorescent chemo sensor for high selectivity and sensitivity of aluminum ions, *Dyes and Pigments*, 2013, **97**, 124-128.
- 8.** S. Goswami, S. Paul and A. Manna, A differentially selective chemosensor for a ratiometric response to Zn^{2+} and Al^{3+} in aqueous media with applications for molecular switches, *RSC Adv.*, 2013, **3**, 25079-25085.
- 9.** S. Sinha, R. R. Koner, S. Kumar, J. Mathew, P. V. Monisha, I. Kazi and S. Ghosh, Imine containing benzophenone scaffold as an efficient chemical device to detect selectively Al^{3+} , *RSC Adv.*, 2013, **3**, 345-351.
- 10.** S. Das, U. Mukherjee, S. Pal, S. Maitra and P. Sahoo, Selective sensing of Al^{3+} ions by nitrophenyl induced coordination: imaging in zebrafish brain tissue, *Org. Biomol. Chem.*, 2019, **17**, 5230-5233.